# 9. Internet of Hearts — Large-Scale Stochastic Network Modeling and Analysis of Cardiac Electrical Signals

Chen Kan and Hui Yang

*Complex Systems Monitoring, Modeling and Analysis Laboratory*
*The Pennsylvania State University*
*310 Leonhard Building*
*University Park, PA 16802*

## Abstract

Rapid advancement of mobile sensing and Internet-of-Things (IoT) technology provides an unprecedented opportunity to realize smart and connected health. However, large-scale IoT systems lead to big data. Realizing the full potential of big data depends on a great extent on the development of new human-centered computing methodologies for real-time health monitoring, on-the-fly disease diagnosis, and timely delivery of life-saving treatments. Thus far, very little has been done to develop advanced IoT technologies for smart monitoring and control of heart health. This chapter presents a new IoT technology of Mobile and E-Network Smart Health (MESH) specific to the heart, also called the Internet of Hearts (IoH), to advance the cardiac mHealth with IoT sensing, stochastic modeling and network analytics. The MESH technology will enable and assist (1) the acquisition of electrocardiogram (ECG) signals pertinent to space-time cardiac dynamics anytime, anywhere; (2) real-time management and compact representation of multi-lead ECG signals; (3) big data analytics in large-scale IoT contexts. In particular, we first developed a spatiotemporal approach to visualize the real-time motion of 3D VCG cardiac vectors. Then, an optimal model-based representation algorithm was developed to facilitate the compression of ECG signals and the extraction of features pertinent to disease-altered signal patterns. Further, we developed stochastic network models for real-time patient-centered monitoring, modeling, and analysis of stochastic variations between heartbeats from an individual and among human subjects. The MESH technology shows a great potential in providing an indispensable and enabling tool for realizing smart heart health and wellbeing for the population worldwide.

## 9.1. Introduction

Cardiac diseases are the leading cause of death in the world. About 30% of global deaths (17.3 million) are due to cardiac diseases. According to the report from World Health Organization (WHO), this number will increase to 23 million by 2030. In United States, heart diseases are responsible for one in every four deaths, amounting to an annual loss of $448.5 billion [1]. Cardiac diseases claim more lives each year than the next four leading causes of death combined — cancer, chronic lower respiratory diseases, accidents, and diabetes mellitus. As opposed to chronic ones, most of the cardiac diseases are acute and can occur at any time in daily life [2]. For example, a heart attack is caused by the blockage in coronary arteries, which results in insufficient blood and oxygen supply to cardiac muscles. When a heart attack occurs, every minute counts. Patients who experience acute heart attacks are required to receive the treatment within 90 minutes after the onset of the symptom. A delay could result in permanent heart muscle damage and increased risk of death. However, if the sign of heart attack is detected early, life-saving medications or treatments can be delivered to avoid hospitalization and even reduce the mortality rate. Therefore, the optimal management and treatment of cardiac diseases hinge on the identification of cardiac disorders in the early stage and the delivery of timely medical interventions.

In the past decade, mobile health (mHealth) has gained increasing attention from the health-care research community. Advances in sensing technology and the rapid expansion of mobile networks have made remotely monitoring of patient's condition and provision of timely feedback possible and affordable. mHealth technologies, therefore, offer a great opportunity to improve diagnosis, treatment, and adherence; increase access to health services, and lower health-care costs. The applications of cardiac mHealth have increased during the recent years. Wireless sensors are readily available to measure single-lead electrocardiogram (ECG). Patients can forward recorded ECG signals to physicians and receive feedbacks remotely. However, the existing mHealth technologies are limited in their ability to analyze complex patterns of ECG signals for the identification of cardiac diseases. This is mainly because the spatiotemporal cardiac electrical activity manifests significant stochastic behaviors. It poses significant challenges on the existing mHealth systems, which implement simple algorithms to recognize disease patterns. It is well known that ECG signals are initiated at the sinoatrial (SA) node, then conducted in both atria, relayed through the atrioventricular (AV) node to further propagate through the bundle of His and Purkinje fibers toward ventricular depolarization and repolarization [3, 4]. Such electrical conduction, nevertheless, is a stochastic process and can be influenced by various types of uncertainties. For example, the excitation of SA node may too slow or too fast, may pause, or fail to exit the SA region. To investigate the underlying mechanisms, researchers developed multiscale recurrence models [5–8] that revealed nonlinear stochastic dynamics in vectorcardiogram (VCG) signals. Furthermore, the process of orchestrated depolarization and repolarization of cardiac muscle cells are controlled by the orchestrated function of individual ion channels in the cell membrane and are, thereby, coupled with real-world uncertainties [9, 10]. Notably, cardiac electromechanical function is closely related to cyclic changes in the differences between intracellular and extracellular concentration of ions. The potential difference increases as multiple ions travel across the cell membrane through ion channels. Ions flow through these channels and, thus, change the action potential across the cell membrane [11, 12]. The rate at which ionic channels open and close is in a stochastic manner and is based largely on the potential difference across the membrane.

The stochastic behavior of the cardiac electrical activity consists of two aspects: within-a-patient and between-patient stochastic dynamics. On the one hand, cardiac electrical activity within a patient demonstrates temporal dynamics. As shown in Fig. 9.1a, a 10-second ECG signal is generated from continuous monitoring. It may be noted that the amplitude of the 4th cycle of the ECG signal is smaller than the first three, so as the 8th cycle. Furthermore, the 6th cycle shows a significant S wave and an elevated T wave. Moreover, apparent variability can be identified even among those cycles that look similar, for example, cycle #1, #2, #3, #9, and #10. The stochastic behavior of cardiac activity for an individual patient is critical to the identification of arrhythmic events. Taking consideration of historical variabilities in cardiac activity is conducive to the delivery of personalized treatment planning. On the other hand, the cardiac activity is different between patients. As shown in Fig. 9.1b, 2-second ECG signals of six patients demonstrate big variability. For example, the heart rate is apparently different among these patients. Patient P1, P3, and P6 have only two ECG cycles, but the others have 2.5–3 cycles within 2 seconds. Also, the morphology of these ECG signals shows significant dissimilarities. Patient P3 shows inverted T wave (i.e., T wave is pointing downward instead of upward). P3 has an abnormal wave before the onsite of Q wave, and the R peak of P6 is notched. Notably, between-patient stochastic behaviors are closely pertinent to the disease-altered cardiac patterns. The detection and differentiation of cardiac diseases hinge on the effective characterization of both within-a-patient and between-patient stochastic behaviors.

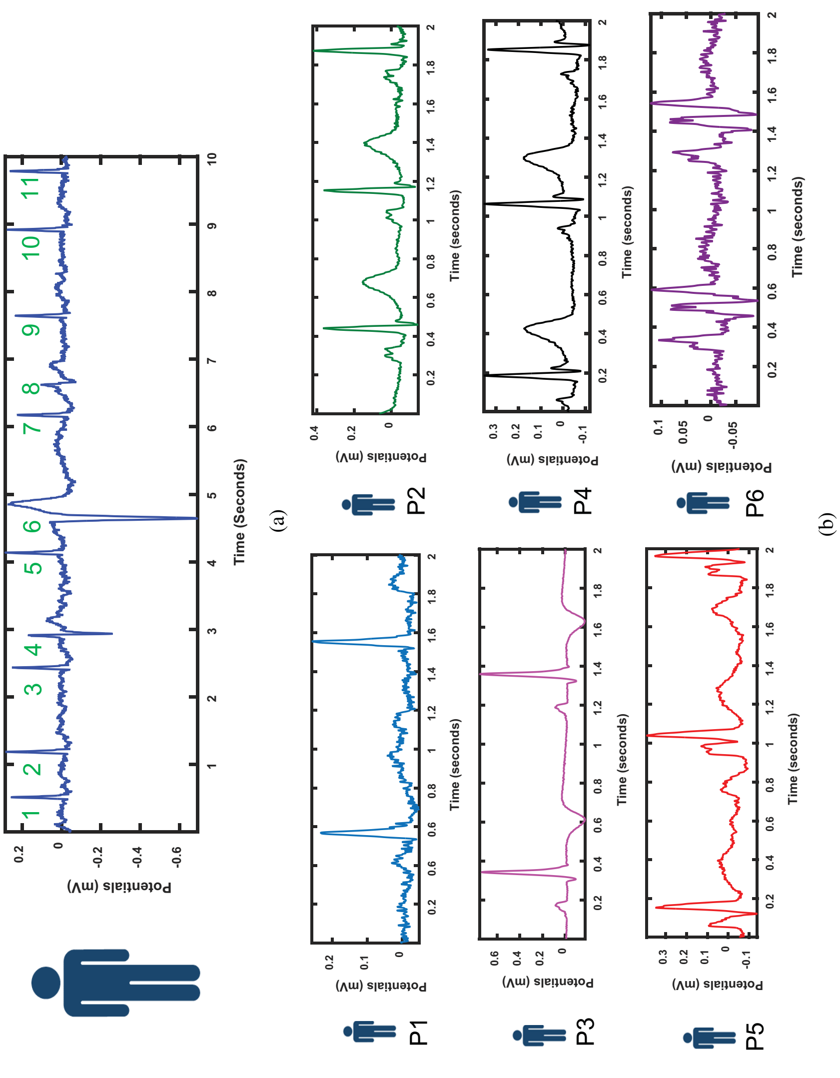


**Figure 9.1.** (a) Within-a-patient and (b) between-patient stochastic behaviors of cardiac electrical activity.

In the present investigation, we developed a new technology of Mobile and E-Network Smart Health (MESH) to advance the cardiac mHealth with stochastic modeling and network analytics [13]. The MESH technology is developed in the world's most widely used iOS mobile operating system, which is compatible with iPhone, iPad, and iPod Touch devices). In addition, it supplies in-situ information processing capabilities and enables physicians to access the patients' ECG signals in real time, remotely interact with the patients, and rapidly respond to life-threatening cardiac disorders. The MESH system is composed of three components: real-time visualization of three-dimensional (3D) VCG trajectory and feature detection, optimal model-based representation of ECG signals, and stochastic network modeling and online diagnosis.

The remainder of this chapter is organized as follows: Section 9.2 presents the background of ECG sensing and signal patterns; Section 9.3 throws light on the present analytical modules for large-scale ECG sensing systems; Section 9.4 provides the design of the MESH system, including the wearable sensor, MESH database, and smart phone applications; Section 9.5 presents marketing research, and Section 9.6 concludes this chapter.

## 9.2. Background

The human heart is essentially an autonomous electro-mechanical blood pump that operates near-periodically to maintain vital living organs. The heart consists of four compartments: right and left atria and right and left ventricles. This autonomous pump circulates blood in the body and constantly produces a sequence of electrical activities within every heartbeat. It is well known that an electrical activity begins in a specified pacemaker region, called the SA node, to excite the atrial muscle contraction. Then, the activity spreads through the upper chambers of the heart (the atria) and reaches the AV node. The AV node propagates the stimulus through bundle of His and Purkinje fibers toward the ventricles [3, 4]. The ordered stimulation, starting from the SA node, leads to the orchestrated contraction of the heart, thereby, pumping the blood throughout the body.

The ECG system, designed by Augustus Waller in 1889 and further improved by Willem Einthoven in 1901, has been used for over 100 years for the monitoring of cardiac electrical activity and clinical diagnosis of cardiovascular disorders [14]. One lead ECG captures one-dimensional (1D) temporal view of a space-time cardiac electrical activity. Multi-lead ECG systems provide multi-directional views of such space-time dynamics [15]. A normal ECG tracing is often segmented into P wave, QRS complex, and T wave (see Fig. 9.2a [16]). Atrial depolarization (and systole) is represented by the P wave, ventricular depolarization (and systole) is represented by the QRS complex, and ventricular repolarization (and diastole) is represented by the T wave [17, 18]. It may be noted that ECG signals contain a wealth of dynamic information pertinent to cardiac operations, which is indispensable for cardiac care — from monitoring and diagnosis to treatment planning to smart health management. Existing time-domain algorithms were developed to quantify the characteristics of ECG wave deflections (i.e., P, QRS, and T waves) for the identification of cardiac diseases. Examples of ECG features

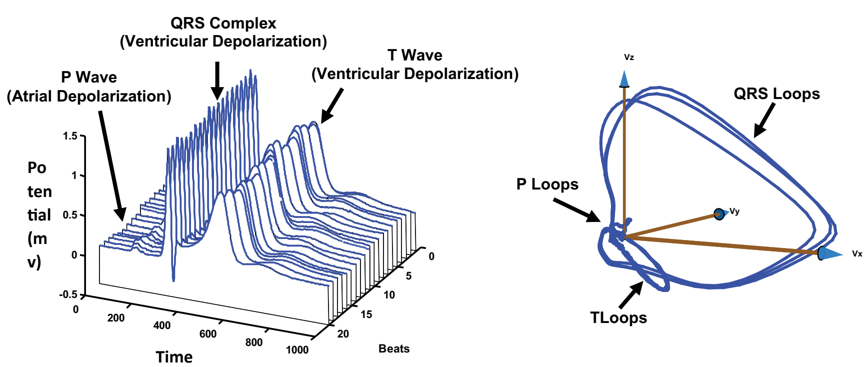


(a) (b)

**Figure 9.2.** Two types of cardiac signals: (a) 2D ECG cycles and (b) 3D VCG loops.

include PR interval, RR interval, ST elevation/depression, QT interval, and R amplitude.

However, time-domain projections of space-time cardiac electrical activity will diminish important spatial information of cardiac pathological behaviors. As such, medical decisions that are made can be significantly influenced by such an information loss [3]. Therefore, 3-lead vector cardiogram (VCG) is designed to provide multi-directional views of space-time electrical activity. VCG observes the heart potentials as a cardiac vector in three orthogonal components instead of the scalar amplitude (ECG curve) [19]. In VCGs, the mutually orthogonal bipolar measurements are taken by placing parallel electrodes on the opposite sides of the torso. As shown in Fig. 9.2b, VCG signals contain P loops, QRS loops, and T loops, which correspond to P wave, QRS complex, and T wave in the ECG, respectively. Dower *et al.* and our previous studies [20–22] have demonstrated that 3-lead VCG can be linearly transformed to 12-lead ECG by multiplying a generalized transformation matrix. Thus, the information in 12-lead ECG is redundant and the 3-lead VCG surmounts not only the information loss in 1-lead ECG but also the redundant information in 12-lead ECG.

In clinical practice, the 12-lead ECG is widely used because physicians are trained and are accustomed to using them. It has, thus, proven its value, time-tested, and considered as the gold standard. It is generally difficult for physicians to interpret disease patterns via the high-dimensional VCGs. However, VCGs capture important space-time information of cardiac electrical activity, which is not contained in ECG signals. The methodologies developed in our previous research were proved to be efficient and effective for identifying disease patterns in VCG signals. Those algorithms have fueled increasing interests in VCG signals. However, they have not been applied to clinical practice due to lack of user-friendly software. Therefore, there is a need to develop software that implements those advanced algorithms. MESH incorporates novel pattern recognition algorithms that will serve as a tool to enable and assist physicians in characterizing VCG patterns and identifying early signs of cardiac disorders. The MESH system not only enables access to patients' data anywhere and anytime but also extracts valuable diagnostic information from the signals to help physicians in the decision-making process. MESH is designed to enable physicians and nurses to access and visualize the patients' ECG signals in real time, as well as timely analysis of patient's data and rapidly respond to life-threatening cardiac disorders.

## 9.3. Analytical Modules

As shown in Fig. 9.3, the proposed MESH system consists of three analytical modules. We first develop a spatiotemporal representation approach to visualize the real-time dynamics of 3D VCG trajectories. This enables physicians and nurses to easily interpret the high-dimensional VCG patterns and extract space-time characteristics. Second, an optimal model-based representation algorithm is developed to facilitate the compression of cardiac signals and extraction of features pertinent to the disease-altered cardiac activity. Third, a stochastic network model is designed for real-time patient-centered

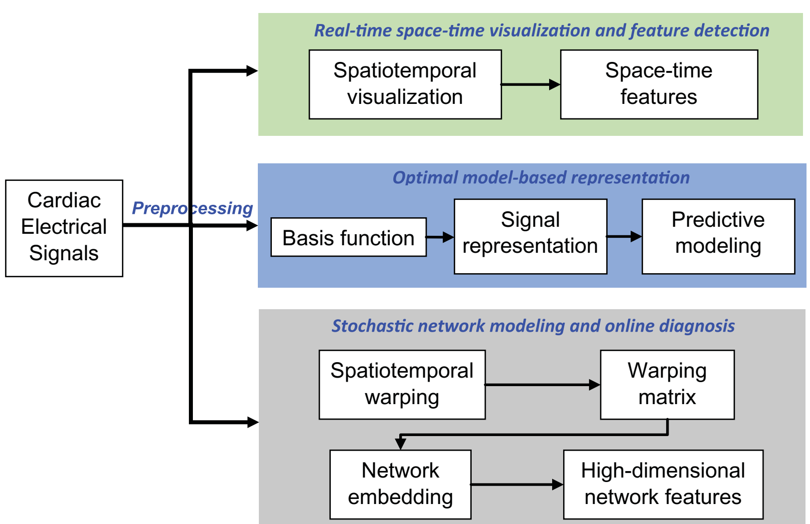


**Figure 9.3.** The overall structure of the proposed MESH system.

monitoring of cardiac variations. The developed spatiotemporal warping algorithm characterizes the patient-patient variations in a warping matrix, which is further embedded into a high-dimensional network to facilitate classification and prediction of patients' cardiac conditions.

### 9.3.1. *Real-time spatiotemporal visualization and feature extraction*

ECG signals are recorded on body surface to track the continuous dynamic details of cardiac functioning. Such valuable real-time information is usually unavailable in static and discrete clinical laboratory tests, for example, computer imaging, chest x-ray, and blood enzyme test. Even if routine laboratory examinations are performed multiple times per day, discontinuity often fails to prevent the lethal consequences of acute cardiac disorders. The awareness about the importance of real-time cardiac monitoring for the early identification pathological patterns is increasing as it tracks cardiac dynamic behaviors, as opposed to static screenshots.

However, lead ECG signals only capture one perspective temporal view of the space-time excitation and propagation of cardiac electrical activities. Multiple lead ECG systems, for example, 12-lead ECG and 3-lead VCG, are designed to capture the multi-directional view of space-time cardiac electrical activities [23]. Time-domain visualization is the traditional routine for representing cardiac electric signals. It is the major function of most of the existing cardiac mHealth systems. The medical doctors are used to the time-domain identification of cardiac disease patterns. Therefore, this module is preserved in MESH. The characteristic points of cardiac signals, for example, locations of R peak and the end of T wave, are automatically detected by implementing the wavelet-based algorithm developed in our previous research.

However, cardiac electrical dynamics are initiated and propagated spatiotemporally. The projection of spatiotemporal activity into 1D time domain diminishes important spatial information underlying cardiac electrical activities. In MESH, a novel dynamic spatiotemporal visualization of VCG signals is implemented [23]. In the Frank XYZ lead system, VCG is represented as three orthogonal scalar measurements with respect to time, which is given as:

$$\begin{cases} v_x = f(t) \\ v_y = g(t). \\ v_z = h(t) \end{cases}$$

The dynamic VCG signal representation embeds the cardiac vector, composed of three scalar measurements, in real time. As shown in Fig. 9.4, three scalar x, y, and z components are plotted in the top and the simultaneous 3D movement of cardiac vectors in the bottom.

The top plot displays VCG signals in three-vector components as a function of time, and the bottom part shows the real-time cardiac vector movement in the 3D space. Head (green) gives the current position of cardiac vector. Body (red) indicates the direction and rotation of cardiac vector movements [23].

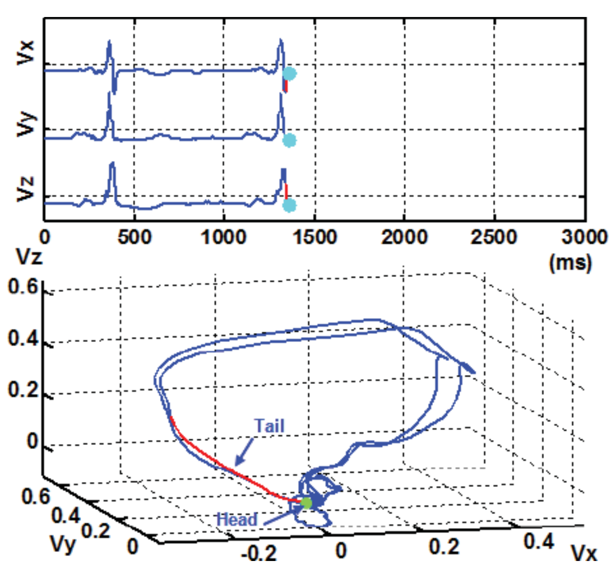


**Figure 9.4.** Real-time spatiotemporal VCG representation.

This explicitly real-time spatiotemporal VCG representation makes it easier to integrate with prior knowledge and experiences of time-based ECG. As shown in Fig. 9.4, this representation consists of three components, namely, head (green), body (red), and tail (blue). Head gives the current position of the cardiac vector. Body records a short history of the cardiac vector movements, which clearly indicates where the current vector is from. It avoids the confusion regarding the group of heart activity to which the current cardiac vector belongs as they usually intersect at the isoelectric points. The tail provides full history pertinent to the complete topological shape of VCG state space. By following the cardiac vector movement with respect to time, the P, QRS, and T waves will be easily located in the VCG state space [23].

The real-time visualization of spatiotemporal ECG signals is an enabling tool that can be used in clinical practices of cardiac care. This approach incorporates additional dynamical properties of cardiac vector movements (such as curvature, velocity, octant, and phase angle) with the color coding scheme, which can be used for the interpretation of high-dimensional cardiac vectors by physicians or nurses. Our prior research [23] showed that the proposed dynamic VCG surmounts some drawbacks of time-domain representation and provides critical spatial, as well as temporal information of the heart dynamics. The cardiovascular pathological patterns are found to be effectively captured by this new 3D dynamic representation approach. The presence of both spatial and temporal characteristics in dynamic representation improves the automatic assessment of cardiovascular diseases with the use of VCG signals.

### 9.3.2. *Optimal model-based representation*

The proposed MESH system enables long-term continuous cardiac monitoring. However, continuous sensing in days, months, and even years generates enormous amount of data, which contains multifaceted information pertinent to the evolving dynamics of process operations. As such, it provides physicians with a spatially and temporally data-rich environment in the process of medical decision-making.

Big data poses significant challenges for human experts (e.g., physicians, nurses, and quality technicians) to accurately and precisely examine all the generated high-dimensional sensor signals for fault diagnosis and quality inspection. Moreover, the proliferation of sensing data also provides an unprecedented opportunity to develop sensor-based methodologies for realizing the full potential of multi-dimensional sensing capabilities toward real-time process monitoring and disease diagnosis.

In MESH, a new model-driven parametric monitoring strategy [16, 24] is developed for the detection of dynamic fault patterns in high-dimensional functional profiles that are non-linear and non-stationary. Specifically, a sparse basis function model is developed to represent high-dimensional functional profiles, which minimizes the number of basis functions involved but maintains sufficient explanatory power. As such, large amount of data is reduced to a parsimonious set of model parameters (i.e., weight, shifting, and scaling factors in basis functions) while preserving the signal information.

The 3D VCG is represented as the superposition of M multiscale basis functions:

$$\vec{v}(t,w) = \vec{w}_0 + \sum_{j=1}^{M} \vec{w}_j \vec{\varphi}_j \left((t-\mu_j)/\sigma_j\right) + \varepsilon,$$

where $\varphi(t)$ is the general basis function form, which is not limited to Gaussian function, $\mu_j$ is the shifting factor, and $\sigma_j$ is the scaling factor. The objective is to minimize the representation error, that is, $\operatorname{argmin}\left[\vec{\boldsymbol{v}}(t) - \vec{\boldsymbol{w}}_0 - \sum_{j=1}^{M} \vec{\boldsymbol{w}}_j \vec{\boldsymbol{\varphi}}_j (t)^2, \{\boldsymbol{w}, M, \boldsymbol{\varphi}(t)\}\right]$, between VCG signals and basis function models. In a matrix form, the basis function model is rewritten as $\boldsymbol{V} = \boldsymbol{W}^T\boldsymbol{\varphi}$, where $\boldsymbol{W}$ is the weight matrix and $\boldsymbol{\varphi}$ is the basis function matrix.

An iterative procedure, that is, matching pursuit algorithms [25], was developed to search the suboptimal solution based on characteristic wave patterns in the VCG/ECG signals. The VCG matching pursuit method is started from an initial approximation $S^{(0)} = 0$, residual $R^{(0)} = \vec{v}(t)$, and dictionary $D = \left\{\varphi_j(t),\ \ j = 1, 2, \ldots, N\right\}$. The first step identifies the basis function in the dictionary that best correlates with the residual, that is, finding $\gamma 0$ such that $\left|R^{(0)}, \varphi^{(\gamma 0)}\right| = \max\left|R^{(0)}, \varphi^{(\gamma)}\right|$, $\gamma \in \mathrm{N}$ and $\varphi^{(\gamma 0)} \in D$. Then, the current approximation will be $s^{(1)} = s^{(0)} + R^{(0)}, \varphi^{(\gamma 0)}\varphi^{(\gamma 0)}$, and the residual is defined as $R^{(1)} = R^{(0)} - R^{(0)}, \varphi^{(\gamma 0)}\varphi^{(\gamma 0)}$. If the orthogonal wavelet bases are used, it may be noted that $\varphi^{(\gamma 0)}$ is orthogonal to $\mathrm{R}^{(1)}$ because:

$$
\begin{aligned}
\varphi^{(\gamma 0)}, R^{(1)} &= \varphi^{(\gamma 0)}, R^{(0)} - R^{(0)}, \varphi^{(\gamma 0)}\varphi^{(\gamma 0)} \\
&= \varphi^{(\gamma 0)}, R^{(0)} - \varphi^{(\gamma 0)}, R^{(0)}, \varphi^{(\gamma 0)}\varphi^{(\gamma 0)} \\
&= \varphi^{(\gamma 0)}, R^{(0)} - R^{(0)}, \varphi^{(\gamma 0)} = 0
\end{aligned}
$$

Hence, $R^{(0)}, \varphi^{(\gamma 0)}\varphi^{(\gamma 0)}$ is also orthogonal to $\mathrm{R}^{(1)}$ so that

$$
R^{(0)2} = R^{(1)2} + R^{(0)}, \varphi^{(\gamma 0)}\varphi^{(\gamma 0)2}
$$

At step j + 1, the residual $\mathrm{R}^{(j+1)}$ is treated as $\mathrm{R}^{(0)}$ in the first step, yielding

$$
R^{(j+1)} = R^{(j)} - R^{(j)}, \varphi^{(\gamma j)}\varphi^{(\gamma j)}
$$

$$
s^{(j+1)} = \sum_{i=1}^{j} R^{(i)}, \varphi^{(\gamma i)}\varphi^{(\gamma i)}
$$

After M such steps, one has a representation of the form of additive decomposition:

$$
v(t) = \sum_{i=1}^{M-1} R^{(i)}, \varphi^{(\gamma i)}\varphi^{(\gamma i)} + R^{(M)}
$$

The adaptive algorithm will stop when the residual sum of squares is less than a small threshold at step M (i.e., $\boldsymbol{R}^{(M)} < \varepsilon$). An intrinsic feature of matching pursuit algorithm is that when the dictionary has orthogonal bases, it works perfectly after a few steps yielding a sparse adaptive representation using only a few basis functions. An example of fitting high-dimensional nonlinear profile using the superposition of basis functions is shown in Fig. 9.5. It may be noted that the basis function model (red/solid) effectively represents the original data (blue/dashed).

It may be noted that optimal representation of 3D VCG topology in the MESH system will lead to the following benefits:

- *Feature extraction*: The model parameters such as weights, shifting, and scaling factors in the basis functions can be potentially used as features for the diagnostic application. As a result, large amount of VCG and ECG data is reduced to a limited amount of features (i.e., model parameters) while preserving the same information.
- *Data compression*: It is well known that hundreds of gigabytes of VCG and ECG data will be stored in the real-time cardiac monitoring. Since the basis function model yields a good representation (>99%) of real-world VCG signals, model parameters can be saved instead of long-term VCG signals.
- *Algorithm evaluation*: This proposed basis function model is data-driven and can be fitted to ECG signals from different kinds of cardiovascular diseases. The fitted model for different pathologies can generate large amount of VCG/ECG signals that can be

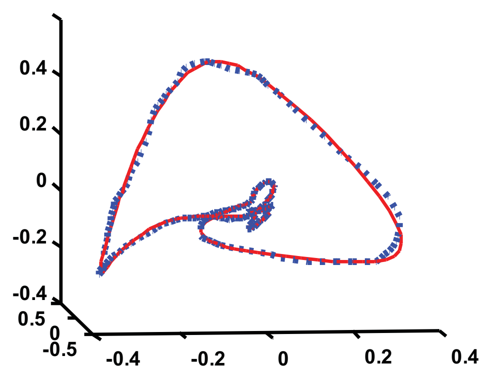


**Figure 9.5.** 3D trajectory of VCG signals from basis function model (red/solid) and real-world data (blue/dashed) [16].

used to test the algorithms of QRST cancellation, adaptive filtering, and classification.

- *Disease prognostics*: Because the basis function model captures all the characteristics from actual data, real-time ECG monitoring signals can be compared with the model representation trained in healthy condition. The differences of pattern similarity can be used as a performance measure for the prognostic purpose.

The model parameters and their derivatives can be used as features for the detection of process faults. However, the dimensionality of these features is high and can potentially lead to sensitive predictive models. Thus, we further utilize lasso-penalized logistic regression model [16] to investigate the "redundancy" and "relevancy" properties between these parameter-based features and fault patterns to identify a sparse set of sensitive predictors from a large number of features for fault diagnostics.

Let $p(\boldsymbol{x}, \boldsymbol{\beta})$ be the probability for $y$ to be a success ($y = 1$) and, thus, $1 - p(\boldsymbol{x}, \boldsymbol{\beta})$ is the probability for $y$ to be a fault ($y = 0$), where $\boldsymbol{\beta} = (\beta_0, \beta_1, \beta_2, \ldots, \beta_p)^T$ is the coefficient vector. The logistic regression model is:

$$\log\left(\frac{p(\boldsymbol{x}, \boldsymbol{\beta})}{1 - p(\boldsymbol{x}, \boldsymbol{\beta})}\right) = \boldsymbol{\beta}^T \boldsymbol{x}$$

The likelihood function of $\boldsymbol{\beta} = (\beta_0, \beta_1, \ldots, \beta_p)^T$, given the observation data $\boldsymbol{X} = (\boldsymbol{x}_1, \boldsymbol{x}_2, \ldots, \boldsymbol{x}_n)^T$, $\boldsymbol{y} = (y_1, \ldots, y_n)^T$ is:

$$\prod_{i=1}^{n} p(\boldsymbol{x}_i, \boldsymbol{\beta})^{y_i} \left(1 - p(\boldsymbol{x}_i, \boldsymbol{\beta})\right)^{1-y_i}$$

As such, the log likelihood function becomes:

$$\begin{aligned} L(\boldsymbol{\beta} | \boldsymbol{X}, \boldsymbol{y}) &= \sum_{i=1}^{n} \left[ y_i \log\left(p(\boldsymbol{x}_i, \boldsymbol{\beta})\right) + (1 - y_i) \log\left(1 - p(\boldsymbol{x}_i, \boldsymbol{\beta})\right) \right] \\ &= \sum_{i=1}^{n} \left[ y_i \boldsymbol{\beta}^T \boldsymbol{x}_i - \log\left(1 + e^{\boldsymbol{\beta}^T \boldsymbol{x}_i}\right) \right] \end{aligned}$$

The lasso-penalized logistic regression is formulated to minimize the following objective function with the constraint that the upper limit of $L_1$-norm of $\boldsymbol{\beta}$ is less than $C$,

$$\min_{\boldsymbol{\beta}} - L\left(\boldsymbol{\beta} \mid \boldsymbol{X}, \boldsymbol{y}\right)$$

$$\text{subject to } \boldsymbol{\beta}_1 \leq C$$

This is equivalent to solve the following unconstrained optimization problem, with $\lambda$ be the regularization parameter:

$$\min_{\boldsymbol{\beta},\lambda} - L\left(\boldsymbol{\beta} \mid \boldsymbol{X}, \boldsymbol{y}\right) + \lambda \boldsymbol{\beta}_1$$

The optimal solution $\boldsymbol{\beta}$ of the unconstrained optimization problem given $\lambda$ also solves the constrained minimization problem with $C = \boldsymbol{\beta}_1 = \sum_{i=1}^{p} \left|\beta_i\right|$. To solve this constrained optimization problem, let us first obtain the solution to the general logistic regression model. The objective function of general logistic regression model is as follows:

$$\min_{\boldsymbol{\beta}} - L\left(\boldsymbol{\beta} \mid \boldsymbol{X}, \boldsymbol{y}\right)$$

From the Newton-Raphson algorithm, it may be noted that the update of parameters is obtained by approximating the objective function with the second-order Taylor expansion. Let $\boldsymbol{\beta}^{(k)}$ be the current parameters, then Newton–Raphson method finds the new set of parameters $\gamma^{(k)}$ based on the quadratic approximation:

$$\boldsymbol{\gamma}^{(k)} = \left(\boldsymbol{X}^T \boldsymbol{W} \boldsymbol{X}\right)^{-1} \boldsymbol{X}^T \boldsymbol{W} \boldsymbol{z},$$

where $\boldsymbol{z} = \boldsymbol{X}\boldsymbol{\beta} + \boldsymbol{W}^{-1}(\boldsymbol{y} - \boldsymbol{p})$ and $W$ is the diagonal matrix with $(\boldsymbol{W})_{ii} = p\left(\boldsymbol{x}_i, \boldsymbol{\beta}\right)\left(1 - p\left(\boldsymbol{x}_i, \boldsymbol{\beta}\right)\right)$. As such, solving for $\gamma^{(k)}$ is equal to finding the solution to the following weighted least squares problem:

$$\boldsymbol{\gamma}^{(k)} = \arg\min_{\boldsymbol{\gamma}} \left(\boldsymbol{W}^{\frac{1}{2}} \boldsymbol{X}\right) \boldsymbol{\gamma} - \boldsymbol{W}^{\frac{1}{2}} \boldsymbol{z}_2^2$$

For lasso-penalized logistic regression, there is a need to add the $L_1$ constraint to the unregularized logistic regression to ensure $\boldsymbol{\gamma}_1 \leq C$, that is,

$$\min_{\gamma} \left( \boldsymbol{W}^{\frac{1}{2}} \boldsymbol{X} \right) \boldsymbol{\gamma} - \boldsymbol{W}^{\frac{1}{2}} \boldsymbol{z}_2^2$$

$$\text{subject to } \boldsymbol{\gamma}_1 \leq C$$

As a result, the lasso-penalized logistic regression is transformed to an iteratively reweighted least square problem. At each iteration, we update the $\boldsymbol{W}^{\frac{1}{2}}\boldsymbol{X}$ and $\boldsymbol{W}^{\frac{1}{2}}\boldsymbol{z}$, based on the new estimate of coefficients. After $\boldsymbol{\gamma}^{(k)}$ is obtained, we update $\boldsymbol{\beta}^{(k)}$ by:

$$\boldsymbol{\beta}^{(k+1)} = (1-\theta)\boldsymbol{\beta}^{(k)} + \theta \tilde{\boldsymbol{a}}^{(k)}$$

where $\theta \in [0,1]$ is the learning rate for the parameter update. In this study, we adopted the coordinate descent algorithm to solve the regularized problem. If we write $\boldsymbol{W}^{\frac{1}{2}}\boldsymbol{X} = \overset{V}{\boldsymbol{X}}$ and $\boldsymbol{W}^{\frac{1}{2}}\boldsymbol{z} = \overset{V}{\boldsymbol{y}}$, only one $\boldsymbol{\beta}_j$ is changed at each time, while the other parameters $\beta_k\,(k \neq j)$ stay the same.

The lasso penalized logistic regression model is implemented in MESH to investigate the "redundancy" and "relevancy" properties between features and fault patterns, thereby identifying a sparse set of sensitive predictors for fault diagnostics. This model was evaluated in our previous study, and the experimental results showed that more than 60% of features had the KS statistic greater than the critical value 0.17, indicating significant differences between control and fault conditions. Furthermore, the lasso-penalized logistic regression model yields a superior accuracy of 97.13%, with a parsimonious set of 81 features. The proposed approach facilitates the modeling and characterization of high-dimensional nonlinear profiles and provides effective predictors for real-time fault detection, thereby promoting the understanding of fault-altered spatiotemporal patterns in the complex cardiovascular systems.

### 9.3.3. *Stochastic network modeling and online diagnosis*

A remarkable feature of MESH is its information-processing capability to perform spatiotemporal recognition of disease patterns using 3D trajectories of cardiac electric signals. As shown in Fig. 9.6, there is spatiotemporal dissimilarity between the 3-lead VCGs of MI (red dashed loops) and HC (blue solid loops) subjects. The quantification of such dissimilarity will provide a great opportunity for the identification of cardiovascular diseases. However, it is challenging to measure the spatiotemporal dissimilarity between two functional signals in both space and time. Due to phase shift and discrete sampling, two VCG signals can be misaligned, for example, both signals show a typical pattern and yet there are variations in shape, amplitude, and phase between them. In the clinical practice, various methods are developed to measure the dissimilarities between misaligned signals. Figure 9.7 illustrates some of them using simple two-dimensional (2D) ECG signals. To compare the ECG signals (blue and red), the intuitive way is to directly take the difference between them (see Fig. 9.7a). As such, the difference may be huge even for similar signal patterns because of the misalignment. For example, the QRS wave (ventricular depolarization) of the blue ECG may be compared to the P wave (atrial depolarization) of the red ECG, which

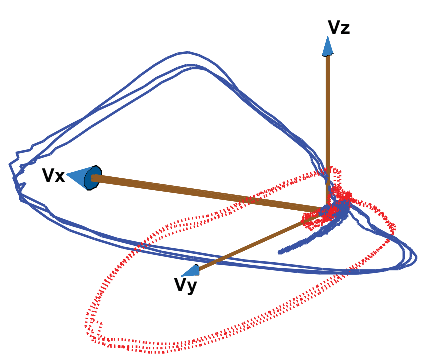


**Figure 9.6.** Spatiotemporal VCG signals of control (blue/solid) and diseased subjects (red/dashed).

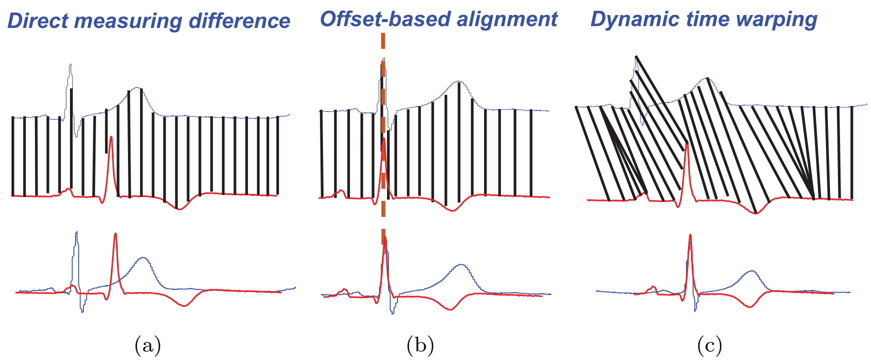


**Figure 9.7.** Measuring dissimilarities between misaligned ECG cycles: (a) Direct difference, (b) Offset based alignment, and (c) Dynamic time warping.

generates misleading results. For years, physicians used offset-based alignment to improve the solution. In other words, R peaks from two ECGs are first aligned together and then take the difference (see Fig. 9.7b). In this way, the ventricular depolarization of two subjects are compared together, but the atrial depolarization (P wave) and ventricular repolarization (T wave) are still misaligned. Finally, dynamic time warping [26, 27] is a viable method that may help optimally align two ECG signals (see Fig. 9.7c). Such an alignment is critical to compare the corresponding electrical activity of heart chambers. For example, we are comparing the ventricular depolarization (i.e., QRS complex) for two subjects, as opposed to the incorrect comparison between atrial depolarization (P waves) from one subject and ventricular depolarization from the other subject.

Importantly, the first step of stochastic network modeling is to implement our dynamic spatiotemporal warping approach to measure the dissimilarities between space-time functional recordings [3, 28]. As opposed to traditional time-domain warping (see Fig. 9.7c), spatiotemporal warping is innovatively created to solve the problem of misalignment in both space and time. As shown in Fig. 9.8, P, QRS, and T loops are aligned for two subjects in both space and time. Notably, little work has been done to measure the differences between VCG loops by means of dynamic time warping. However, 3-lead VCG signals are analogous to the voice from the heart.

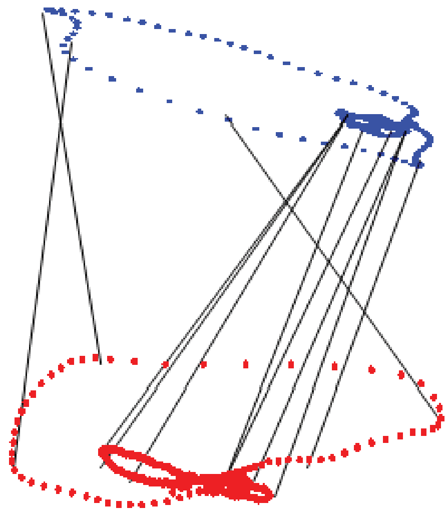

**Figure 9.8.** Spatiotemporal alignment of 3-lead VCG signals [3].

Our algorithm is the first of its kind to utilize space-time warping of VCG signal patterns for the identification of disease patterns and has been granted two patents [29, 30].

Given two 3D VCG signals $\overrightarrow{\boldsymbol{v}_1}(t)$ and $\overrightarrow{\boldsymbol{v}_2}(t)$, the time-normalized spatial distance between $\overrightarrow{\boldsymbol{v}_1}(t)$ and $\overrightarrow{\boldsymbol{v}_2}(t)$ is calculated as $\sum_{(t_i,t_j)\in p} \overrightarrow{\boldsymbol{v}_1}(t_j) - \overrightarrow{\boldsymbol{v}_2}(t_j)$ by alignment $p$. The warping path $p(i, j)$ connects (1, 1) and $(N_1, N_2)$ in a 2D square lattice as well as satisfying constraints such as monotonicity condition and step size condition. To find the optimal path, an exhaustive search of alignment path is intractable and computationally expensive. However, this problem is solved efficiently using dynamic programming (DP) methods. The DP algorithm is started at the initial condition: $g(1,1) = d(1,1) = \overrightarrow{\boldsymbol{v}_1}(t_1) - \overrightarrow{\boldsymbol{v}_2}(t_1)$ and the warping window $|i - j| < r$. The algorithm is searching forward as follows:

$$g(i,j) = min\begin{pmatrix} g(i,\ j-1) +\ d(i,\ j) \\ g(i-1,\ j-1) +\ d(i,\ j) \\ g(i-1,\ j) +\ d(i,\ j) \end{pmatrix}$$

Finally, the time-normalized spatial distance is calculated as follows:

$$\Delta\left(\overrightarrow{\boldsymbol{v}_1}, \overrightarrow{\boldsymbol{v}_2}\right) = \frac{g\left(N_1, N_2\right)}{N_1 + N_2}$$

where $N_1$ and $N_2$ are the length of $\overrightarrow{\boldsymbol{v}_1}(t)$ and $\overrightarrow{\boldsymbol{v}_2}(t)$, respectively. The $\Delta\left(\overrightarrow{\boldsymbol{v}_1}, \overrightarrow{\boldsymbol{v}_2}\right)$ represents the spatiotemporal dissimilarity between two multidimensional functional recordings. Therefore, disease-altered characteristics of 3-lead VCG signals are obtained in the warping matrix.

However, it may be noted that the warping matrix itself cannot be used as features for the identification of disease properties in classification models. In addition, the measure of Euclidean distance is not directional and can mix the distances that are equal in magnitudes but along different spatial directions. A novel method needs to be developed to transform the warping matrix into feature vectors that preserve the warping distances among functional recordings. The spatial embedding method represents the functional recordings as the points in a high-dimensional space. These points can be used as feature vectors that recover not only the distance matrix but also directional differences between functional recordings [28].

This is similar to a network problem, that is, how to reconstruct the location of nodes in a high-dimensional space if the node-to-node distance matrix is known. As shown in Fig. 9.8, a network comprises a number of nodes that are connected by edges. Each node stands for an individual component in the system, and the edges show the relationship (e.g., distances or causal relationships) between nodes. As given in Fig. 9.9a, assume the distance matrix $\Delta$ for five nodes is known. If the network is reconstructed in the 3D space, this is analogous to optimally identify the coordinate vector $\boldsymbol{x}_i = (x_{i1}, x_{i2}, x_{i3}),\ i = 1,2,\ldots,5$ for five nodes that can preserve the distance matrix $\Delta$. As shown in Fig. 9.9b, all the nodes and their connections preserve the dissimilarities matrix $\Delta$. The matrix $D$ is the pairwise distances between reconstructed nodes in the 3D space.

$$\Delta = \begin{bmatrix} 0 & 5 & 4.5 & 5.5 & 4 \\ 5 & 0 & 3.5 & 6 & 3.5 \\ 4.5 & 3.5 & 0 & 5.5 & 4.5 \\ 5.5 & 6 & 5.5 & 0 & 5 \\ 4 & 3.5 & 4.5 & 5 & 0 \end{bmatrix}$$

(a)

$$D = \begin{bmatrix} 0 & 5.01 & 4.37 & 5.54 & 3.76 \\ 5.01 & 0 & 3.02 & 6.00 & 2.87 \\ 4.37 & 3.02 & 0 & 5.45 & 4.53 \\ 5.54 & 6.00 & 5.45 & 0 & 4.88 \\ 3.76 & 2.87 & 4.53 & 4.88 & 0 \end{bmatrix}$$

(b)

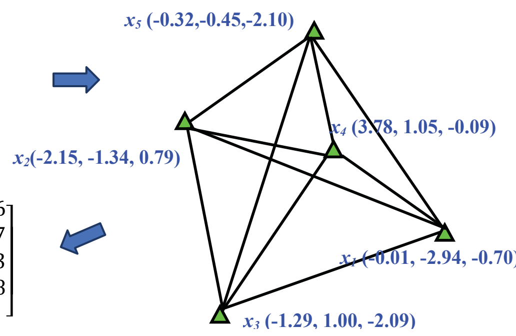


(c)

**Figure 9.9.** (a) Original distance matrix Δ, (b) reconstructed network and nodes in the 3D space, and (c) reconstructed distance matrix D [3].

It may be noted that we are bridging from functional signals to the distance matrix to feature vectors (nodes in the network). The feature vectors will approximately preserve the distance matrix Δ between functional signals.

Let u assume that $\delta_{ij}$ denotes the dissimilarity between $i^{\text{th}}$ and $j^{\text{th}}$ functional recordings in $n \times n$ warping matrix Δ, $x_i$, and $x_j$ denotes the $i^{\text{th}}$ and $j^{\text{th}}$ feature vectors in a high-dimensional space. Then, the objective function of feature embedding algorithm can be formulated as follows:

$$\min \sum_{i<j} (\boldsymbol{x}_i - \boldsymbol{x}_j - \delta_{ij});\ i, j \in [1, n]$$

where Δ is the Euclidean norm. To solve this optimization problem, the Gram Matrix $B$ is firstly reconstructed from the $n \times n$ distance (dissimilarity) matrix Δ:

$$B = -\frac{1}{2} H \Delta^{(2)} H$$

where the centering matrix $H = I - n^{-1} 11^T$ and **1** is a column vector with $n$ ones. The $\Delta^{(2)}$ is a squared matrix and each element in $\Delta^{(2)}$ is

$\delta_{ij}^2$ (i.e., the squares of $\delta_{ij}$ in the matrix $\Delta$). The element $b_{ij}$ in matrix $B$ is:

$$b_{ij} = -\frac{1}{2}\left[\delta_{ij}^2 - \frac{1}{n}\sum_{k=1}^{n}\delta_{ik}^2 - \frac{1}{n}\sum_{k=1}^{n}\delta_{kj}^2 + \frac{1}{n^2}\sum_{g=1}^{n}\sum_{h=1}^{n}\delta_{gh}^2\right]$$

It is known that the Gram Matrix $B$ is defined as the scalar product $B = XX^T$, where the matrix $X$ minimizes the aforementioned objective function. The Gram Matrix $B$ can be further decomposed as $B = V\Lambda V^T = V\sqrt{\Lambda}\sqrt{\Lambda}V^T$, where $V = [\boldsymbol{v}_1, \boldsymbol{v}_2, \ldots, \boldsymbol{v}_n]$ is a matrix of eigenvectors and $\Lambda = \text{diag}(\lambda_1, \lambda_2, \ldots, \lambda_n)$ is a diagonal matrix of eigenvalues. Then, the matrix of feature vectors is obtained as $X = V\sqrt{\Lambda}$. The algorithm embeds each functional recording as a feature vector in the $d$-dimensional space ($d = 2, 3, 4, \ldots$).

To this end, a network is optimally constructed in the high-dimensional space. Notably, such network is not static. It is a dynamic network that contains both within-a-patient and between-patient stochastic behaviors. For example, each cycle of the 10-second ECG signal from an individual patient (see Fig. 9.1a) is represented as a node in the network. It may be noted that the node location is changing over time due to the cycle-to-cycle stochastic dynamics. As shown in Fig. 9.10, network nodes are located closely when ECG cycles have similar morphology. However, when there is a significant change, for example, cycle #6, the node moves far away from the previous cycles. Such stochastic network reveals the cycle-to-cycle dynamics and provides physicians useful information pertinent to the underlying changing of cardiac conditions of an individual patient.

Figure 9.11 demonstrates the stochastic network for different patients. Like Fig. 9.10, two nodes are distributed closely when two patients share similar cardiac conditions. The positions of nodes are changing if cardiac conditions vary with respect to time. For example, when patient P1 also gets myocardial infarction symptoms as P3, the corresponding node will move toward P3. As such, physicians are quickly alerted and deliver life-saving therapies in time.

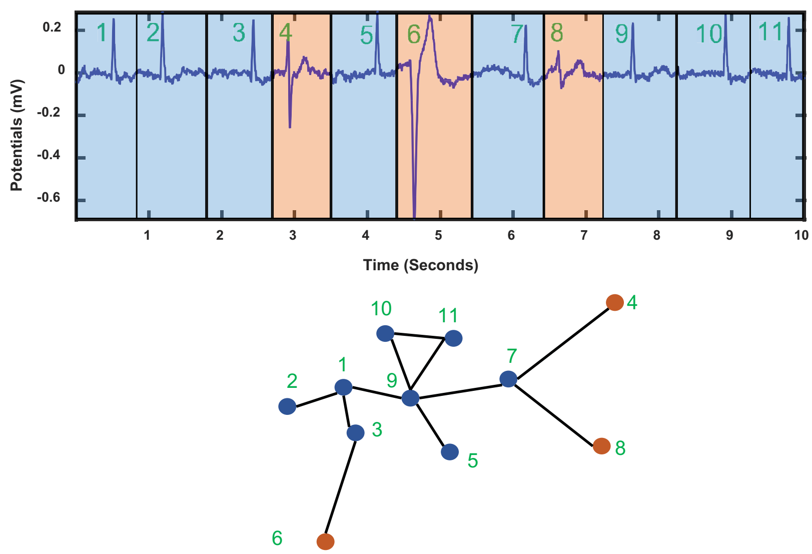


**Figure 9.10.** Stochastic network for monitoring cycle-to-cycle dynamics of an individual patient.

The proposed stochastic network model can be readily used for online diagnosis. As shown in Fig. 9.12, when a new VCG recording is presented, the pattern dissimilarity will be measured against the database of $N$ patients. Then, a new row and column will be obtained in the warping matrix, and a new feature vector will be embedded in the high-dimensional space. Finally, the classification model will predict cardiac conditions with this feature vector [31].

However, the large number of patients in MESH poses great challenges for real-time analytics and management. On one hand, MESH is aimed at integrating patients all over the world to reduce the risk of cardiac diseases and improve the quality of life. More than 17.5 million people die from cardiac diseases every year, and this number is expected to grow to over 23.6 million by 2030. It is extremely expensive to process millions and billions of patients and provide feedbacks within a reasonably short time. On the other hand, MESH is aimed at long-term monitoring of patients' cardiac

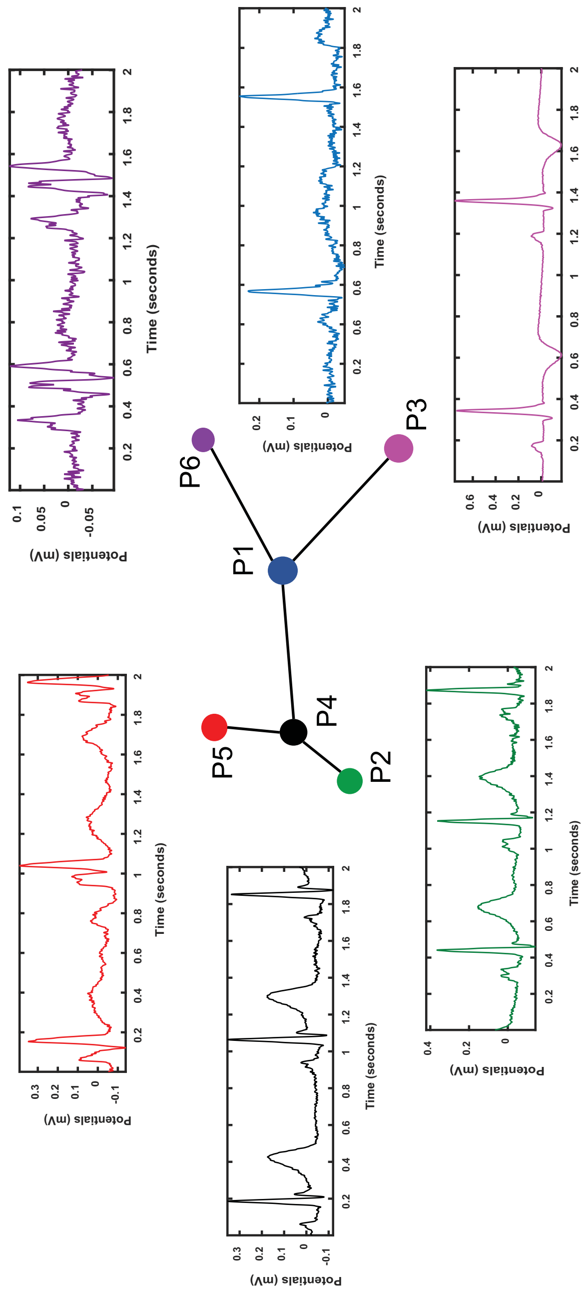


**Figure 9.11.** Stochastic network for monitoring patient-to-patient dynamics.

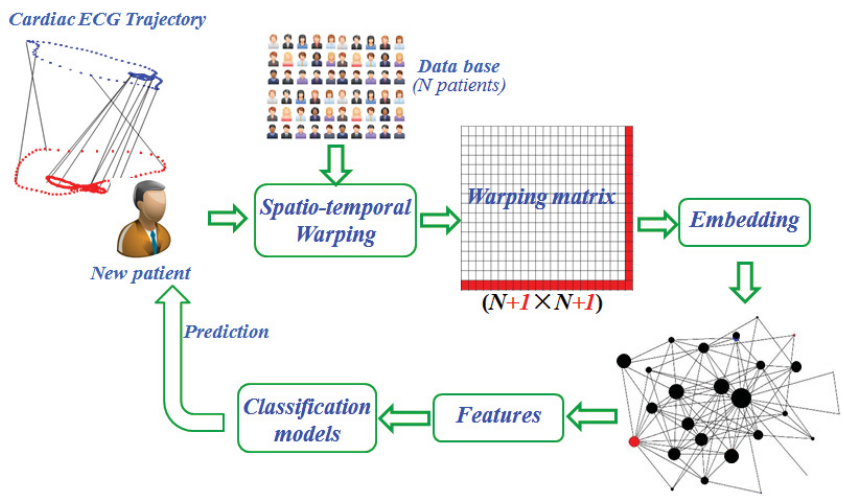


**Figure 9.12.** The flowchart of stochastic network modeling and online diagnosis.

conditions for personalized cardiac care. Continuous monitoring of an individual patient generates a large amount of data when performed in hours, days, months, and years. There is lack efficient tools to handle such ever-increasing volume of data.

Therefore, we further have developed a new map-reduce framework in MESH for large-scale computing. That is, we have decomposed the large-scale stochastic network optimization problem into local networks and resolved them in a parallel manner [32]. By applying stochastic gradient descent, local networks are optimally casted. Then, the global stochastic network is built by optimally piecing together the local ones. Notably, the proposed strategy facilitates the implementation of parallel computing on a multitude of processors and significantly improve the computation efficiency of the MESH system.

## 9.4. MESH Design

As shown in Fig. 9.13, the proposed MESH system integrates wearable ECG sensors and mobile computing with network analytics for smart heart health management. The wearable sensing device will

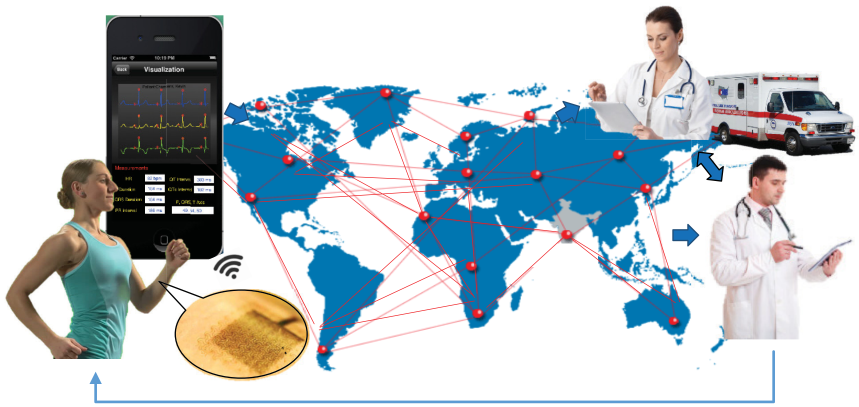

**Figure 9.13.** The overall framework of the designed MESH prototype [32].

continuously monitor cardiac conditions. Patients will be able to install the *MESH App* onto their smartphones and tablets to register and get connected to the system. After proper authorization, physicians will be able to access patients' data, review results in each analytical module, and communicate with patients and other physicians for timely cardiac care.

In the past decade, the Internet of Things (IoT) was hailed as a revolution in health care. The IoT system deploys a multitude of wireless sensors, mobile computing units, and physical objects in an Internet-like infrastructure. This provides an unprecedented opportunity to realize a smart automated system that consists of medical devices and analytical modules to advance connected cardiac care. Connected care has been advocated by the Office of the National Coordinator for Health Information Technology for years. As opposed to traditionally isolated care, a highly connected cardiac care system resembles a large-scale network, which seamlessly connects physicians, patients, devices, databases, and other entities. Optimizing the connectivity in cardiac care provides a data-rich environment for medical decision-making, enables smart cardiac telehealth, facilitates personalized patient-centered care, and diminishes care disparities.

However, most of the existing products focus on wearable sensing and fitness applications while being limited in the capability for cardiac sensing and clinical applications. Very little work has been done to develop advanced IoT technologies for smart monitoring and maintain heart health. Therefore, the proposed MESH system is developed to fill this gap. MESH is a new IoT technology specific to the heart, and it is aimed at realizing the next-generation of the cardiac mobile health system (namely the *Internet of Hearts*), proposed by our research group.

### 9.4.1. *Wearable sensing device*

The existing electrodes are foam-made, fixed-shape, and attached to the skin by electrolyte gel. They do not adhere well to the irregular body surface, thereby, resulting in artifacts during body movement. In this study, we have exploited microdevices assembled on stretchable substrates to develop a new generation of ECG sensors that can stretch, fold, twist, and wrap around the complex surface of the skin. Furthermore, we embedded wireless module (e.g., Bluetooth LE) into the ECG sensor. Thin film circuits of the wireless module were patterned on the soft material so that they can accommodate to large deformations. Moreover, the skin-like substrate architecture quantitatively reproduces mechanics of the non-linear property of the real skin. This, in turn, significantly improved the wearability and facilitate unobtrusive long-term monitoring. As shown in Fig. 9.14a, stretchable sensors have been developed to measure EMG signals in the state of the art [33, 34]. Also, we have developed an ECG sensing board with Bluetooth LE module (Fig. 9.14b) to wirelessly transmit sensing data to mobile devices [13].

Furthermore, the sensor-skin contact can be oftentimes influenced by sweating, motion, among other factors. Thus, the contact is not only static but also dynamic. Notably, the performance of ECG sensors with microelectrodes deteriorates significantly in dynamic contact. As such, the segments of ECG signals or even an entire lead can be missing. In other words, it is not uncommon to

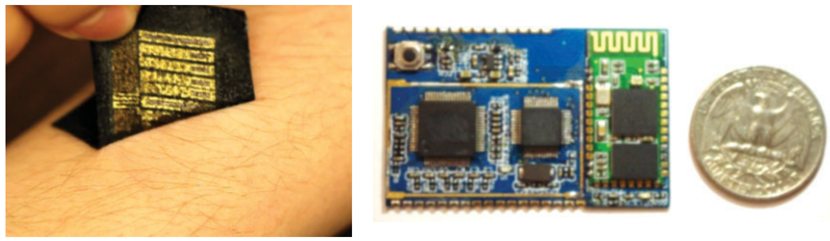

(a) (b)

**Figure 9.14.** (a) Stretchable bio-sensors [33, 34], (b) Wireless ECG sensing board.

encounter sensor failures in body area sensor networks. For example, a subset of sensors often loses contact with the skin surface in ECG sensor networks because of body movements. Maintaining strict skin contacts for hundreds of sensors is not only challenging but also greatly deteriorates the wearability of ECG sensor networks. Therefore, we have proposed a novel strategy, named stochastic sensor network, which allows a subset of sensors at varying locations within the network to transmit dynamic information intermittently [35]. Notably, the new strategy of stochastic sensor networks is generally applicable in many other domains. For example, a wireless sensor network is often constrained by finite energy resources. Hence, optimal scheduling of activation and inactivation of sensors is imperative to realize long-term survivability and reliability of sensor networks. This information-theoretic approach is integrated with sparse particle filtering to impute missing ECG segments and compensate missing lead(s). In our previous study, we implemented sparse particle filtering for modeling space-time dynamics in an cardiac activity with stochastic sensor networks. The wearable sensing device of MESH will yield an efficient hardware-software solution to ensure the extraction of sufficient diagnostic information from ECG sensor networks.

### 9.4.2. *MESH database*

An advanced cloud database, that is, MESHDB, is developed to store user data of the proposed MESH system. The cloud platform optimally allocates the memory among the cluster of servers, which enable nearly unlimited space for storage. At the same time, the MESH system will protect the information stored in the MESHDB. The objective of data management is to specifically focus on optimal management and handling of cyber security issues of cloud database. Notably, the MESH system will only allow the use of MESH app (please refer to Section 9.4.3 for details) and the cloud database from registered users. The users will also be allowed to add notes for each patient and send alert information to the care group. In addition, MESH is designed to connect to ECG data management systems hosted in each hospital. For example, GE MUSE system is a central database that stores all the patients' data and information in the cardiology unit at hospitals. The GE MUSE system provides rich information on cardiology assessments, making administrative workflow and sharing and securing information.

The MESH technology will realize smart and connected cardiac health, once it is available to everyone in the world. It is well-known that the large-scale database is critical to big data analytics, which has the potential to transform the next-generation health care [36]. Big data presents a "gold mine" of this era (21st century). Toward this end, cardiac health care in the future is envisioned to be equipped with the mobile technology, mobile-based data acquisition and cloud database and big data analytics. With new wearable ECG sensing devices, users can directly collect and upload cardiac signals to the MESH system. Each recording will be automatically analyzed by MESH and stored in a cloud database. The more users involved, the bigger the database is, the more powerful the MESH will be. Notably, low-dimensional embedding of a large-scale network can include millions of patients around the world.

Figure 9.15 shows the data flow in the MESH system. Note the arrows indicate the direction of data flows. Primary physicians and care providers in hospitals and home care services have access to their assigned patients in the GE MUSE database hosted by hospitals and home care facilities, as well as in the cloud database hosted by MESH. They can review real-time cardiac recordings for analysis and send back instant feedbacks and care alerts. This will greatly

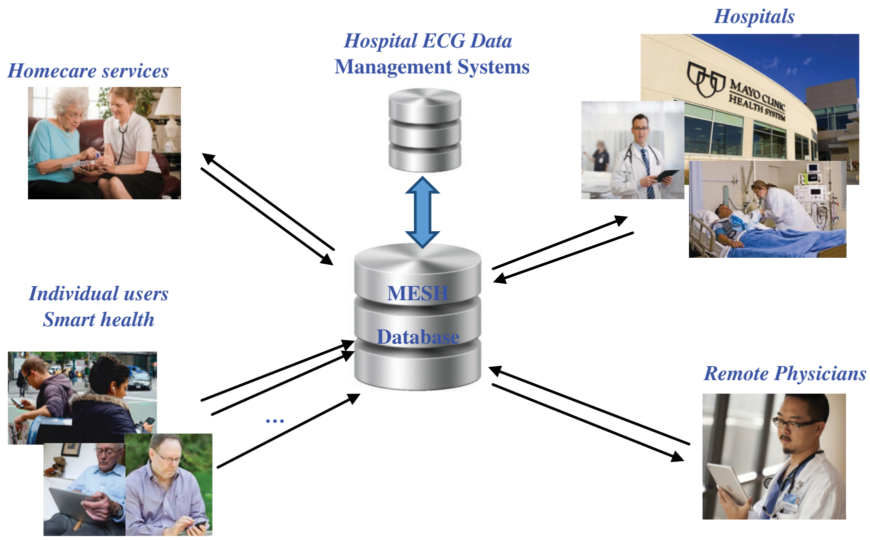


**Figure 9.15.** Database design of the proposed MESH system.

promote early identification and diagnosis of life-threatening cardiac events (e.g., heart attacks and cardiac arrest). Furthermore, if the patient wants to seek diagnosis results and treatment advice from cardiac experts all around the world, the MESH system can also enable remote physicians to review and analyze the patient's data. In this way, better treatments of cardiovascular diseases can be achieved by teamed efforts from physicians with different background and expertise. Individual users worldwide will be able to monitor their cardiac electric activity in real time, upload data into the cloud database, and consult the physician online. It should be noted that MESH realizes the patient-centered cardiac care anywhere and anytime with the mobile technology and the internet. It is expected that the MESH system will provide an indispensable enabling tool for realizing smart health and wellbeing for the population worldwide.

### 9.4.3. *MESH smartphone application*

We have developed a mobile application to implement partial functions of the proposed MESH system. This application is developed in the world’s most widely used iOS mobile operating system (which is compatible with iPhone, iPad, and iPod Touch devices). It enables physicians to access the patients’ ECG signals in real time, remotely interact with patients, and rapidly respond to life-threatening cardiac disorders.

Screenshots of designed MESH application are shown in Fig. 9.16. Figure 9.16a–c guide the user through login and patient selection. First, the Login page allows the authorized users to enter their username and password to log into the MESH system. This guarantees the security of the data stored in MESH and protects the privacy of the users. Then, the users such as physicians will be directed to the Sites page that lists hospitals and homecare services. The patients’ profiles and data are categorized by the hospital or homecare service. The user can select one site to list his/her assigned patients associated

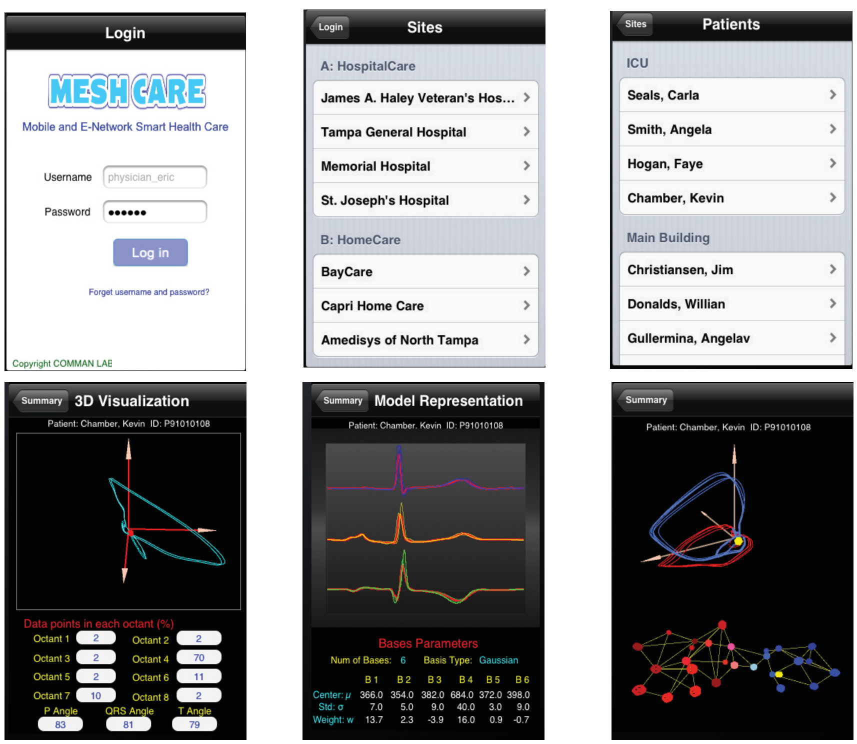


Figure 9.16. Screenshots of designed MESH APP on iPhone.

with that site. On the Patients page, all patients associated with the selected healthcare site are listed. Patients are organized by their categories. If a patient is not shown in the list, the doctor needs to go back and select the correct healthcare site. This can be done by clicking on the Sites button on the navigation bar.

Figure 9.16d–f demonstrate three major functions of the MESH system, that is, dynamic visualization of space-time VCG signals, optimal model-based representation, and stochastic network analytics. On "3D visualization" page, dynamic space-time VCG signals are displayed on the upper panel. The red point gives the current position of the cardiac vector. The cyan loops record the full history pertinent to complete the topological shape of the VCG state space. The plot is automatically rotating counter-clockwise on the z-axis. The rotation facilitates a $360^{\circ}$ view of spatiotemporal signals. Spatiotemporal features are updated in real time in the lower panel, including the percentage of data points in each of the eight octants, and the angle of P, QRS, and T axis.

On "Model Representation" page, multiple cycles are collected from each of the three VCG channels and displayed on the upper panel (blue → X channel, yellow → Y channel, and green → Z channel). The red curves (with large line width) are the basis function models obtained from the summation of six adaptive Gaussian functions. It is noteworthy that the models effectively capture the morphology of signals. The parameters of basis functions, including center, standard deviation, and weight, are listed in the lower panel for basis 1 (B1) to basis 6 (B6).

On the last page, that is, dynamic network analytics, 3D visualization of VCG loops are shown in the upper panel. The blue trajectory is from a normal subject, and the red trajectory is from myocardial infarction. The yellow indicator moving along the VCG cycles represents the current cycle we are looking at. The plot is automatically rotating counter-clockwise on the z-axis, providing a $360^{\circ}$ view of spatiotemporal cardiac patterns. The embedded network is displayed on the lower panel. Nodes are the patients in the database: red nodes are myocardial infarction patients and blue nodes are healthy subjects. The yellow node in the network indicates the current position of the patient (e.g., Kevin Chamber in this screenshot). When the yellow indicator in the upper panel is moving along the blue cycles, the yellow node on the lower panel is within the group of healthy subjects (i.e., blue nodes). However, when the yellow indicator in the upper panel moves into the red cycles, the yellow node in the network is switched to the cluster of myocardial infarction patients (i.e., red nodes).

## 9.5. Discussion

The developed MESH system is aimed at a large market for patient-centered cardiac care. In 2013, more than 83.3 million American adults (>1 in 3) had heart diseases. The increasing prevalence of cardiac disease calls for smarter cardiac care services. The growing presence of smartphones and tablets provides an unprecedented opportunity to advance cardiac telemedicine and realize the smart cardiac care anytime anywhere, which is not only responsive but also cost effective.

In the NSF I-Corps program, which aimed at developing entrepreneurial skills to translate research results from academic laboratories, we did an extensive marketing research regarding the developed MESH system. We interviewed over 100 cardiac patients, physicians, and cardiac nurses; identified unprecedented marketing opportunities; and found the following:

(1) There is a lack of wireless sensing devices for continuous monitoring of multi-channel ECG signals. The existing companies are developing portable cardiac monitors, which can only monitor a single-channel ECG and are limited in their ability to facilitate the diagnosis of complex cardiac disorders in the clinical practice. Furthermore, most of the existing monitors adopt dry electrodes. It is uncomfortable to take daily activity with them, and they may result in skin irritation. The proposed MESH system is not only able to record hospital-grade multi-lead ECG, but also comfortable, flexible, and reliable to facilitate long-term continuous monitoring.

(2) Currently, there is a great shortage of physicians in the United States, and this situation will worsen in the next decade. Patients with acute cardiac disorders need 24/7 monitoring, but physicians cannot stay in hospitals or with the patients all the time. Currently, when doctors are outside hospitals, they ask nurses to take pictures of ECG signals and send them through the phone. This is apparently not an efficient approach because certain delays are unavoidable, and the resolution of pictures is limited. Equipped with advanced cloud database, the proposed MESH system can be ready to help physicians access patients' data anywhere and anytime to give a timely diagnosis and medical intervention.

(3) There is a lack of enabling tools to extract useful information from big data that is generated from continuous cardiac monitoring. Early identification of disease patterns hinges on information-processing and data mining algorithms. The existing devices are only capable of extracting simple ECG characteristics or transferring data to physicians for visual inspection. MESH innovatively adopts stochastic network analytics for disease pattern recognition. Unlike traditional warping that can only be used to align signals in time domain, the proposed method is able to quantify the space-time dissimilarities between 3D trajectories of cardiac signals. One remarkable feature of the MESH system is that it considers both within-a-patient and between-patient stochastic dynamics for network-based pattern recognition of cardiac diseases. This will assist and enable physicians in the decision-making process.

## 9.6. Summary

Cardiovascular diseases are the leading cause of death around the world. According to WHO, cardiac diseases contribute to more than 30% of the global deaths each year. Optimal management and treatment of cardiac diseases hinge on the development of advanced cardiac telemedicine system for the detection of fatal disease patterns in the early stage and timely delivery of life-saving therapies. However, the cardiac electrical activity manifests significant stochastic properties in both space and time. The existing approaches are either not concerned with underlying changes of cardiac conditions for an individual patient or not capable to effectively differentiate different cardiac conditions among patients. There is an urgent need to fully address underlying stochastic properties and uncertainties in the cardiac electrical activity.

This chapter presents new visualization and data analytics tools for stochastic modeling and analysis of cardiac electrical signals, which advance cardiac telehealth-care service with exceptional features such as personalization, responsiveness, and superior quality. Specifically, we first developed a spatiotemporal approach to capture space-time heart dynamics by displaying the real-time motion of 3D VCG cardiac vectors. Then, an optimal model-based representation algorithm was developed to facilitate the compression of cardiac signals and the extraction of features pertinent to the disease-altered cardiac activity. Then, a stochastic network model was designed for real-time patient-centered monitoring, modeling, and analysis of cardiac variations. Finally, we leveraged the developed algorithms and built the next-generation cardiac mHealth system, MESH.

MESH bridges gaps in the current cardiac telemedicine systems and serves as an enabling tool to reduce the risk of life-threatening cardiac disorders and deliver personalized therapies.

We expect that this chapter will spur further investigations in stochastic modeling and analysis of spatiotemporal ECG signals to accelerate the discovery of knowledge in cardiovascular research.

## Acknowledgment

This work is supported in part by the National Science Foundation (CMMI-1646660 and CMMI-1617148). The authors also thank Harold and Inge Marcus Career Professorship (HY) for additional financial support.

## References


1. Roger, VL, AS Go, DM Lloyd-Jones, EJ Benjamin, JD Berry, WB Borden, DM Bravata, S Dai, ES Ford, CS Fox, HJ Fullerton, C Gillespie, SM Hailpern, JA Heit, VJ Howard, BM Kissela, SJ Kittner, DT Lackland, JH Lichtman, LD Lisabeth, DM Makuc, GM Marcus, A Marelli, DB Matchar, CS Moy, D Mozaffarian, ME Mussolino, G Nichol, NP Paynter, EZ Soliman, PD Sorlie, N Sotoodehnia, TN Turan, SS Virani, ND Wong, D Woo and MB Turner (2012). Heart disease and stroke statistics — 2012 update. *Circulation,* 125(1), e2–e220.
2. Jaffe, A, L Babuin and F Apple (2006). Biomarkers in acute cardiac disease. *J. Am Coll Cardiol.,* 48(1), 1–11.
3. Yang, H, C Kan, G Liu and Y Chen (2013). Spatiotemporal differentiation of myocardial infarctions. *IEEE Trans Autom Sci Eng.,* 10(4), 938–947.
4. Chen, Y and H Yang (2012). Self-organized neural network for the quality control of 12-lead ECG signals. *Physiol. Meas.,* 33(9), 1399.
5. Chen, Y and H Yang (2013). A comparative analysis of alternative approaches for quantifying nonlinear dynamics in cardiovascular system. In *2013 35th Annual International Conference of the IEEE Engineering in Medicine and Biology Society (EMBC)*, 2013, 2599–2602.
6. Yang, H (2011). Multiscale recurrence quantification analysis of spatial cardiac vectorcardiogram signals. *IEEE Trans Biomed Eng.,* 58(2), 339–347.
7. Chen, Y and H Yang (2013). Wavelet packet analysis of disease-altered recurrence dynamics in the long-term spatiotemporal vectorcardiogram (VCG) signals. In *2013 35th Annual International Conference of the IEEE Eng Med Biol Soc.,* 2013, 2595–2598.
8. Chen, Y and H Yang (2012). Multiscale recurrence analysis of long-term nonlinear and nonstationary time series. *Chaos Solitons Fract.,* 45(7), 978–987, 7.
9. Qu, Z, G Hu, A Garfinkel and J Weiss (2014). Nonlinear and stochastic dynamics in the heart. *Physics Reports,* 543(2), 61–162.
10. Lerma, C, T Krogh-Madsen, M Guevara and L Glass (2007). Stochastic aspects of cardiac arhythmias. *J Stat Phys.,* 128, 347–374.
11. Du, D, H Yang, SA Norring and ES Bennett (2014). In-silico modeling of glycosylation modulation dynamics in hERG ion channels and

cardiac electrical signals. *IEEE J Biomed Health Informat.*, 18(1), 205–214.

12. Du, D, H Yang, H Yang H, AR Ednie and ES Bennett (2015). Statistical metamodeling and sequential design of computer experiments to model glyco-altered gating of sodium channels in cardiac myocytes. *IEEE J Biomed Health Informat.*, PP(99), 1–12.
13. Kan, C, Y Chen, F Leonelli and H Yang (2015). Mobile sensing and network analytics for realizing smart automated systems towards health internet of things. In *2015 IEEE International Conference on Automation Science and Engineering* (*CASE*), pp. 1072–1077. Gothenburg: IEEE Conference Publications. [24–28 August 2015].
14. Malmivuo, J and R Plonsey (1995). *Bioelectromagnetism: Principles and Applications of Bioelectric and Biomagnetic Fields*. New York: Oxford University Press.
15. Dale, D (2000). *Rapid Interpretation of EKG's: An Interactive Course*. Tampa, FL: Cover Publishing Company.
16. Liu, G, C Kan, Y Chen and H Yang (2014). Model-driven parametric monitoring of high-dimensional nonlinear functional profiles. In *2014 IEEE International Conference on Automation Science and Engineering* (*CASE*), pp. 722–727. Taipei: IEEE Conference Publications. [18–22 August 2014].
17. Yang, H, STS Bukkapatnam and R Komanduri (2007). Nonlinear adaptive wavelet analysis of electrocardiogram signals. *Physical Review E*, 76, 026214.
18. Bukkapatnam, S, R Komanduri, V Yang, P Rao, WC Lih, M Malshe, LM Raff, B Benjamin and M Rockley (2008). Classification of atrial fibrillation (AF) episodes from sparse electrocardiogram (ECG) datasets. *J Electrocardiol.*, 41(4), 292–299.
19. Yang, H, STS Bukkapatnam, T Le and R Komanduri (2011). Identification of myocardial infarction (MI) using spatio-temporal heart dynamics. *Med. Eng. Phys.*, 34(4), 485–497.
20. Dower, GE, A Yakush, SB Nazzal, RV Jutzy and CE Ruiz (1988). Deriving the 12-lead electrocardiogram from four (EASI) electrodes. *J Electrocardiol.*, 21(1), S182–S187.
21. Dower, GE and HB Machado (1979). XYZ data interpreted by a 12-lead computer program using the derived electrocardiogram. *J Electrocardiol.*, 12(3), 249–261.
22. Dawson, D, H Yang, M Malshe, STS Bukkapatnam, B Benjamin and R Komanduri (2009). Linear affine transformations between 3-lead

(Frank XYZ leads) vectorcardiogram and 12-lead electrocardiogram signals. *J Electrocardiol.,* 42(6), 622–630.

23. Yang, H, STS Bukkapatnam and R Komanduri (2012). Spatiotemporal representation of cardiac vectorcardiogram (VCG) signals. *Biomed Eng Online,* 11(12), 16.
24. Liu, G and H Yang (2013). Multiscale adaptive basis function modeling of spatiotemporal vectorcardiogram signals. *IEEE J Biomed Health Informatics,* 17(2), 484–492.
25. Mallat, SG and Z Zhang (1993). Matching pursuits with time-frequency dictionaries. *IEEE Trans Signal Process.,* 41(12), 3397–3415.
26. Jeong, Y, MK Jeong and OA Omitaomu (2011). Weighted dynamic time warping for time series classification. *Pattern Recognition,* 44, 2231–2240.
27. Myers, C, L Rabiner and A Rosenberg (1980). Performance tradeoffs in dynamic time warping algorithms for isolated word recognition. *IEEE Trans Acoustics Speech Signal Process.,* 28(6), 623–635.
28. Kan, C and H Yang (2012). Dynamic spatiotemporal warping for detection and location of myocardial infarctions. In *The Eighth Annual IEEE International Conference on Automation Science and Engineering* (*CASE 2012*), pp. 1046–1051. Seoul, Korea: IEEE Conference Publications. [20–24 August 2012].
29. Yang, H (2013). Systems and methods for determining a cardiovascular condition of a subject. US Patent No. 14036776.
30. Yang, H (2013). Systems and methods for diagnosing cardiovascular conditions. International PCT patent No.61700575.
31. Yang, H and F Leonelli (2016). Self-organizing visualization and pattern matching of vectorcardiographic QRS waveforms. *Comput Biol Med.,* 79, 1–9.
32. Kan, C, FM Leonelli and H Yang (2016). Map reduce for optimizing a large-scale dynamic network — Internet of hearts. In *Proceedings of 2016 IEEE Engineering in Medicine and Biology Society Conference* (*EMBC*), pp. 1–4. Orlando, FL: IEEE Conference Publications.
33. Cheng, H, Y Zhang, K Hwang, J Rogers and Y Huang (2014). Buckling of a stiff thin film on a pre-strained bi-layer substrate. *Int J Solids Structures,* 51(18), 3113–3118.
34. Jang, K, H Chung, S Xu, CH Lee, H Luan, J Jeong, H Cheng, GT Kim, SY Han, JW Lee, J Kim, M Cho, F Miao, Y Yang, HN Jung, M Flavin, H Liu, GW Kong, KJ Yu, SI Rhee, J Chung, B Kim, JW Kwak,

MH Yun, JY Kim, YM Song, U Paik, Y Zhang, Y Huang and JA Rogers (2015). Soft network composite materials with deterministic and bio-inspired designs. *Nature Communications*, 6, 6566.

35. Chen, Y and H Yang (2016). Sparse modeling and recursive prediction of space–time dynamics in stochastic sensor networks. *IEEE Trans Automation Sci Eng.*, 13(1), 215–226.
36. Yang, H and E Kundakcioglu (2014). Healthcare intelligence: Turning data into knowledge. *IEEE Intelligent Syst.*, 29(3), 54–68.